Organosulfur derivatives of the HDAC inhibitor valproic acid sensitize human lung cancer cell lines to apoptosis and to cisplatin cytotoxicity

ARTICLE *in* JOURNAL OF CELLULAR PHYSIOLOGY · OCTOBER 2012

Impact Factor: 3.84 · DOI: 10.1002/jcp.24039 · Source: PubMed

Journal of Cellular Physiology

Organosulfur Derivatives of the HDAC Inhibitor Valproic Acid Sensitize Human Lung Cancer Cell Lines to Apoptosis and to Cisplatin Cytotoxicity

ANNA TESEI,[1]* GIOVANNI BRIGLIADORI,[1] SILVIA CARLONI,[1] FRANCESCO FABBRI,[1] PAOLA ULIVI,[1] CHIARA ARIENTI,[1] ANNA SPARATORE,[2] PIERO DEL SOLDATO,[3] ALICE PASINI,[4] DINO AMADORI,[5] ROSELLA SILVESTRINI,[1] AND WAINER ZOLI[1]

[1]*Biosciences Laboratory, IRCCS Istituto Scientifico Romagnolo per lo Studio e la Cura dei Tumori (I.R.S.T.), Meldola, Italy*

[2]*Dipartimento di Scienze Farmaceutiche "Pietro Pratesi," Università degli Studi di Milano, Milan, Italy*

[3]*CTG Pharma, Milan, Italy*

[4]*Laboratory of Cellular and Molecular Engineering, University of Bologna, Cesena Campus, Cesena, Italy*

[5]*Department of Medical Oncology, Istituto Scientifico Romagnolo per lo Studio e la Cura dei Tumori (I.R.S.T.), Meldola, Italy*

Lung cancer is the leading cause of cancer mortality worldwide and despite efforts made to improve clinical results, continuing poor survival rates indicate that novel therapeutic approaches are needed. Valproic acid (VPA), a short-chain branched fatty acid used mainly for the treatment of epilepsy and bipolar disorder, has been shown to inhibit class I histone deacetylases (HDAC-I), a group of enzymes involved in chromatin remodeling and which are thought to play a role in tumor development. Although evidence of VPA's therapeutic efficacy has also been observed in patients with solid tumors, the very high concentration required to induce antitumor activity limits its clinical usefulness. We used a panel of NSCLC cell lines to evaluate the activity and mechanisms of action of organosulfur valproic acid derivatives, a promising new class of compounds designed to improve the safety and efficacy of the valproic acid molecule and created by coupling it with a hydrogen sulfide (H_2S)-releasing moiety. Our results highlighted the increased cytotoxic activity of the novel organosulfur derivatives, ACS33 and ACS2, with respect to VPA, starting from low concentrations. In particular, ACS2 exhibited important pro-apoptotic activity triggered by the mitochondrial pathway and also showed anti-invasion potential. Furthermore, our in vitro results identified a highly effective combination schedule of ACS2 and cisplatin capable of inducing a synergistic interaction even when the two drugs were used at low concentrations, which could prove a valid alternative to traditional chemotherapeutic regimens used for advanced lung cancer. Further studies are needed to confirm these preliminary findings.

J. Cell. Physiol. 227: 3389–3396, 2012.

Lung cancer is the leading cause of cancer mortality worldwide with nearly one million deaths occurring each year (Spiro and Porter, 2002; Parkin et al., 2005; Spiro and Silvestri, 2005). Despite efforts during the past few years to improve clinical results, little more than 10% of patients with non-small cell lung cancer (NSCLC) are still alive at 5 years, of whom only 2% with stage IIIB–IV tumors (Ibrahim et al., 2005). Although innovative biological treatments and new combinations of conventional cytotoxic drugs have been developed, new molecules are urgently needed.

It has long been recognized that cell chromatin patterns, which are morphological markers of the epigenome, are important features of normal and pathological processes. The appearance and quality of chromatin are therefore routinely used to distinguish between normal and neoplastic cells in human specimens. There is increasing evidence that chromatin remodeling through the acetylation and deacetylation of nucleosome core proteins regulates transcriptional activation and repression. Such remodeling is now considered to be as important as mutations or chromosomal alterations in tumors, especially as numerous epigenetic changes precede the development of invasive cancer (Jenuwein and Allis, 2001; Feinberg and Tyco, 2004; Marks et al., 2004; Baylin and Ohm, 2006; Feinberg et al., 2006). It has been also hypothesized that epigenetic-mediated alterations could be the driving force behind chemotherapy resistance, whether intrinsic or acquired. The fact that epigenetic and chromatin changes in tumor cells are potentially reversible, unlike DNA sequence mutations, makes chromatin modifiers promising anticancer therapeutic agents.

The acetylation/deacetylation of histone tails, a form of chromatin pattern modification, is strictly regulated by the members of two important enzyme families: histone acetyltransferases (HAT) and histone deacetylases (HDAC). The classic human HDAC family consists of 11 members divided into three classes (I, II, and IV) with non-redundant

Abbreviations: VPA, valproic acid; NSCLC, non-small cell lung cancer; HDAC, histone deacetylase.

Conflicts of interest: The authors have no conflicts of interest to declare.

*Correspondence to: Anna Tesei, Istituto Scientifico Romagnolo per lo Studio e la Cura dei Tumori (I.R.S.T.), via P. Maroncelli 40, 47014 Meldola (FC), Italy. E-mail: anna.tesei@irst.emr.it

Manuscript Received: 11 November 2011
Manuscript Accepted: 16 December 2011

Accepted manuscript online in Wiley Online Library (wileyonlinelibrary.com): 29 December 2011.
DOI: 10.1002/jcp.24039

functions in normal development and cancer biology. In tumor tissues, the expression of distinct HDAC family members is upregulated and correlates with clinical outcome (Witt et al., 2008). In particular, class I HDACs are considered the most important enzymes for anticancer drug targeting. The term "HDAC inhibitors" is commonly used for compounds that target classes I, II, and IV HDACs, which are frequently used in clinical trials (Witt et al., 2008). Valproic acid (VPA) is a short-chain branched fatty acid that is widely used as an anticonvulsant and mood-stabilizing drug, especially for the treatment of epilepsy and bipolar disorder. Recently, it has also been shown to inhibit class I HDACs 1, 2, 3, and 8 (Marchion et al., 2005) and has proven promising in combination with demethylating agents in clinical studies on hematological cancers (McIntyre et al., 2007). Encouraging results have also been obtained in patients with solid tumors, including breast cancer and melanoma, and studies are ongoing to evaluate VPA for the treatment of glioblastoma and NSCLC (Duenas-Gonzalez et al., 2008). However, the major drawback of VPA is the very high concentration required to induce antitumor activity.

In an effort to improve the safety and efficacy of this drug, a hydrogen sulfide (H_2S)-releasing moiety was coupled to the molecule of valproic acid, obtaining a new, promising class of compounds. The rationale behind this strategy was mounting evidence that H_2S plays a pivotal cell signaling role and is now emerging as a potentially important mediator of cell growth (Baskar and Bian, 2011), cardiovascular homeostasis and cytoprotection (Benavides et al., 2007). Furthermore, several epidemiologic and experimental carcinogenesis studies have shown that components of garlic, including the H_2S-releasing moiety, have anticancer properties against various tumor histotypes, including colorectal, prostate, and lung cancers. In particular, dithiolthiones, oltipraz, anethole trithione, and S-methyl methanethiosulfonate are known to exert anti-cancer effects (Reddy, 1996; Reddy et al., 1999; Kensler et al., 2000; Ruggeri et al., 2002). On this basis, organosulfur derivatives of valproic acid have been synthesized and studied in in vitro and in vivo experimental models of prostate cancer (Wedel et al., 2008) and NSCLC (Perrino et al., 2008; Moody et al., 2010), revealing enhanced antiproliferative activity and HDAC inhibitory properties compared to the parent compound.

The present study focuses on the antitumor activity of novel organosulfur valproic acid derivatives, used as single agents or in combination with conventional antineoplastic drugs, in a panel of human tumor cell lines derived from different NSCLC histotypes.

Materials and Methods

Cell lines

The study was performed on established cell lines representative of different human NSCLC histotypes: CAEP, derived from an epidermoidal carcinoma, established and characterized in our laboratory (Gasperi-Campani et al., 1998), ChaGo-K1, a bronchiogenic cell line, and NCIH1915, derived from a metastatic brain lesion of a lung adenocarcinoma and purchased from the American Type Culture Collection. Cells were maintained as a monolayer at 37°C and subcultured weekly. Culture medium was composed of DMEM/HAM F12 (1:1) supplemented with fetal calf serum (10%), glutamine (2 mM), non-essential amino acids (1%) (Mascia Brunelli S.p.A., Milan, Italy), and insulin (10 μg/ml) (Sigma Aldrich, Milan, Italy). Cells were used in the exponential growth phase for all of the experiments.

Drugs

Valproic acid derivatives ACS2, ACS33 were prepared as previously described (Fig. 1) (Isenberg et al., 2007; Perrino et al., 2008). ACS2 was solubilized in PEG 400 because of its poor solubility in aqueous solution, while ACS33 and valproic acid were dissolved in DMSO (Carlo Erba, Milan, Italy) to a concentration of 100 mmol/L, divided into aliquots and stored at −80°C. Drug stocks were freshly diluted in culture medium before each experiment. Final DMSO and PEG 400 concentrations never exceeded 1% and 0.5%, respectively, and these conditions were used as controls in each experiment.

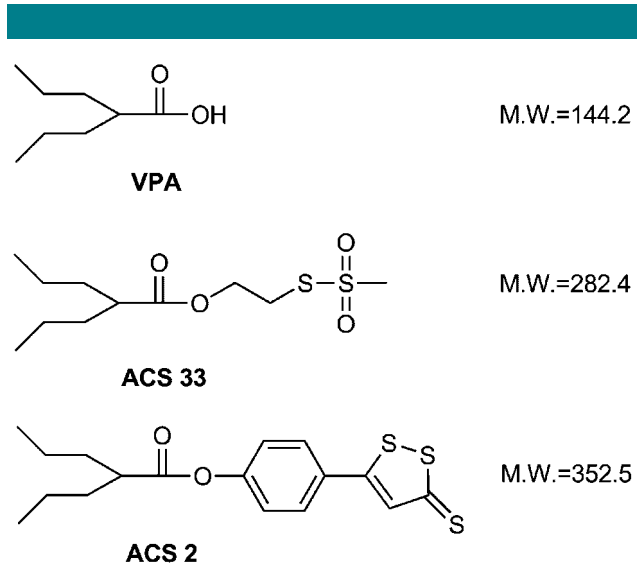

Fig. 1. Chemical structure and molecular weight (M_w) of valproic acid, its H2S-derivative, ACS33, and ACS2.

Chemosensitivity assay

The sulforhodamine B (SRB) assay was used according to the method of Skehan et al. (1990). Briefly, cells were collected by trypsinization, counted, and plated at a density of 5,000 per well in 96-well flat-bottomed microtiter plates (100 μl cell suspension/well). Experiments were run in octuplet and each experiment was repeated thrice. The absorbance of treated cells was determined at a wavelength of 540 nm using a colorimetric plate reader.

Single drug exposure

Valproic acid, ACS2, and ACS33 were tested singly at concentrations of 1, 35, 70, 140, 210, 280 μM for 72 h. Dose response curves were created by Excel software and the 50% inhibiting concentration (IC_{50}) values were determined graphically from the plots.

Drug combination exposure

Different drug schedules were used: (a) simultaneous exposure to ACS2 and cisplatin for 6 h followed by ACS2 for 66 h; (b) exposure to the sequence ACS2 for 72 h → cisplatin for 6 h → 18-h washout; and (c) the inverse sequence, i.e., cisplatin for 6 h → 18-h culture in drug-free medium → ACS2 for 72 h. In all drug combination experiments, ACS2 and cisplatin were tested at concentrations of 70, 140, 210, and 280 μM. Furthermore, appropriate controls were included in the experimental design and in the data analysis to calculate the interaction between the different treatment schedules (e.g., ACS2 and cisplatin for 6 h followed by a 66-h wash-out; ACS2 for 66 h, cisplatin for 6 h followed by a 90-h wash-out, etc.).

The following drug schedules were used for the combination studies with ACS2 and doxorubicin (DOXO): (a) DOXO (1 h) → w.o. (71 h) → ACS2 (72 h); (b) ACS2 (72 h) → DOXO (1 h) → w.o. (71 h); (c) ACS2 + DOXO (1 h) → ACS2 (71 h). In all

these experiments, ACS2 was tested at concentrations of 70, 140, 210, and 280 μM, while doxorubicin was used at concentrations of 0.005, 0.05, 0.5, and 5 μM.

For data analysis, several methods have been proposed to evaluate the interaction between drugs, as critically analyzed by Zoli et al. (2001). However, most of these are not applicable to drugs with a low cytotoxic effect or to those lacking dose-response curves, as in the case of cisplatin. We therefore used Kern et al.'s method (1988) subsequently modified by Romanelli et al. (1998) to overcome this problem. In brief, the expected cell survival (S_{exp}, defined as the product of the survival observed with drug A alone and the survival observed with drug B alone) and the observed cell survival (S_{obs}) for the combination of A and B were used to construct an R index (RI): $RI = S_{exp}/S_{obs}$. $RI > 1.5$ indicated a synergistic interaction, $RI < 0.5$, antagonism and $RI \geq 0.5$ and ≤ 1.5, additivity.

Flow cytometric analysis

TUNEL assay. At the end of drug exposure, the percentage of apoptotic cells was evaluated by flow cytometric analysis according to the previously described TUNEL assay procedure (Rosetti et al., 2006). Briefly, after treatment cells were trypsinized, fixed, exposed to the TUNEL reaction mixture, counterstained with propidium iodide, and then analyzed by FACS.

Mitochondrial membrane potential ($\Delta\Psi$) depolarization assay. After a 72-h exposure to ACS2 140 μM, mitochondrial membrane potential was evaluated by flow cytometric analysis according to the previously described JC-1 method (Rosetti et al., 2006). Data acquisition and analysis were performed using CELLQuest software. 15,000 events were recorded for each sample.

Cytochrome c release assay. Cells were treated according to the manufacturer's instructions (Inno Cyte™ Flow Cytometric Cytochrome c Release Kit, Calbiochem®, EMD Chemicals, Inc., Darmstadt, Germany). Briefly, cells were washed once in PBS and then immediately incubated in permeabilization buffer for 10 min on ice, fixed in 8% paraformaldehyde and washed twice with 1× wash buffer. Cells were then incubated with anti-cytochrome c antibody diluted 1:1,000 in blocking buffer for 1 h, washed and incubated with anti-IgG FITC diluted 1:300 in blocking buffer, according to the manufacturer's instructions. Cells were then resuspended in 1× wash buffer and analyzed using a FACSCanto flow cytometer (Becton Dickinson, San Diego, CA).

DNA denaturation assay. DNA denaturability was probed using acridine orange (AO), the metachromatic fluorochrome which differentially stains double-stranded (ds) versus single stranded (ss) DNA sections (Darzynkiewicz, 1994). AO, when bound to ds DNA, yields green fluorescence, whereas its interaction with ss DNA results in red fluorescence (Darzynkiewicz and Kapuscinski, 1990). The fluorescence color of DNA-bound AO shows the status of DNA denaturation, which in turn, correlates with chromatin condensation.

Briefly, cells were fixed with 1% formaldehyde in PBS on ice, then treated with RNAse A (MP Biomedicals, 5 Kunitz units/ml) and exposed to 0.1 M HCL for 30 sec at room temperature. Cells were subsequently stained with AO (10 μg/ml) (Sigma) dissolved in 0.1 M citric acid-phosphate buffer at pH 2.6. Data were analyzed by flow cytometry using a FACSCanto flow cytometer (Becton Dickinson, San Diego, CA) and experiments were repeated twice.

Western blot analysis

Cells were treated according to the previously described Western blot procedure (Rosetti et al., 2006). The following primary antibodies were used: anti-caspase-3 and anti-caspase-9 (Cell Signaling Technology, Inc., Celbio, Pero, Milan, Italy), anti-acH3 and anti-acH4 (Upstate Millipore, Milan, Italy), β-actin (Santa Cruz Biotechnology, Inc-DBA., Segrate, Italy). Densitometric analysis of the bands was performed by Image Lab software (BioRad).

Matrigel invasion assay

Invasion assays were performed in triplicate in 24-well multiwell plates containing BD Falcon Cell Culture inserts with 8-μm filters coated with Matrigel basement membrane matrix (BD Biosciences, Milan, Italy). NIH 3T3 cells were used as control cells. After drug exposure, each well was loaded with 10×10^4 cells and incubated for 22 h at 37°C in 5% CO_2 atmosphere. Non-invasive cells were removed from the upper surface of the membrane with a cotton swab. The invasive cells on the underside of the membrane were fixed in 100% methanol and stained with 1% toluidine blue. The air dried membrane was placed on a slide and cells were counted under light microscope at 40× magnification. The percentage of invasion was calculated according to the manufacturer's instructions.

Quantitative real-time PCR

PCR Real Time was performed for MMP1 using TaqMan Gene Expression Assay and for housekeeping genes, HPRT1 and GAPDH, using TAqMan Universal PCR Master Mix, No AmpErase UNG (Applied Biosystems, Monza, Italy). PCR reactions were carried out in triplicate on 7500 PCR Real Time System (Applied Biosystems) under the following conditions: 95°C for 10 min, and 40 cycles at 95°C for 15 sec and 60°C for 1 min. The data obtained were analyzed by AbiPrism 7000 software. Reproducibility of RT-PCR was verified in triplicate reactions and the coefficient of variation (CV), calculated from three Ct values, was always <1.5%.

Statistical analysis

Differences between treatments in terms of dose-response, apoptosis and gene expression modulation were determined using the Student's *t*-test for unpaired observations. $P < 0.05$ was considered significant.

Results

Cytotoxic activity

The activity of valproic acid and its derivatives ACS33 and ACS2 in all cell lines after a 72-h exposure to different concentrations is shown in Figure 2A. Valproic acid did not cause a significant reduction in cell survival, whereas both ACS33 and ACS2 showed cytotoxic activity. In particular, ACS2 proved to be the most active compound in all cell lines as it resulted in survival rates falling to below 50% at concentrations ranging from 64.5 to 72 μM (Fig. 2B).

TUNEL assay analysis showed apoptosis induction of about 30% in ChaGo-K1 and about 60% in NCIH1915 and CAEP cell lines after a 72-h exposure to ACS2 140 μM, (Fig. 3A). After the same exposure time, cleavage of the active forms of pro-caspases-9 and -3 (Fig. 3B) and a strong depolarization of mitochondrial membrane potential (Fig. 3C) were also observed. Concomitantly, similar releases of cytochrome c (around 50%) were seen in all three cell lines (Fig. 3D).

To determine whether ACS2 possesses anti-invasive activity, we examined its effect on the invasion potential of a highly metastatic human lung cancer line, NCIH1915 using the Matrigel invasion assay. After a 72-h exposure to 140 μM, ACS2 inhibited the potential invasion of NCIH1915 cells by about 30% (Fig. 4A) and also caused a significant reduction in MMP1 expression levels (Fig. 4B).

We also investigated the interaction between ACS2 and cisplatin after different simultaneous or sequential exposure schedules (Table 1). The sequence cisplatin → ACS2 with an intermediate washout showed an additive interaction in NCIH1915 and CAEP cells, but an antagonistic effect in ChaGo-K1 line. The inverse sequence produced an additive interaction in all three cell lines. Conversely, a strong synergistic interaction was observed in all cell lines after simultaneous exposure to ACS2 and cisplatin for 6 h followed by a continuous 66-h exposure to ACS2 (Table 1, Fig. 5). In particular, simultaneous exposure to both drugs led to a decrease in cell survival in all cell lines starting from the lowest dose used. This was most

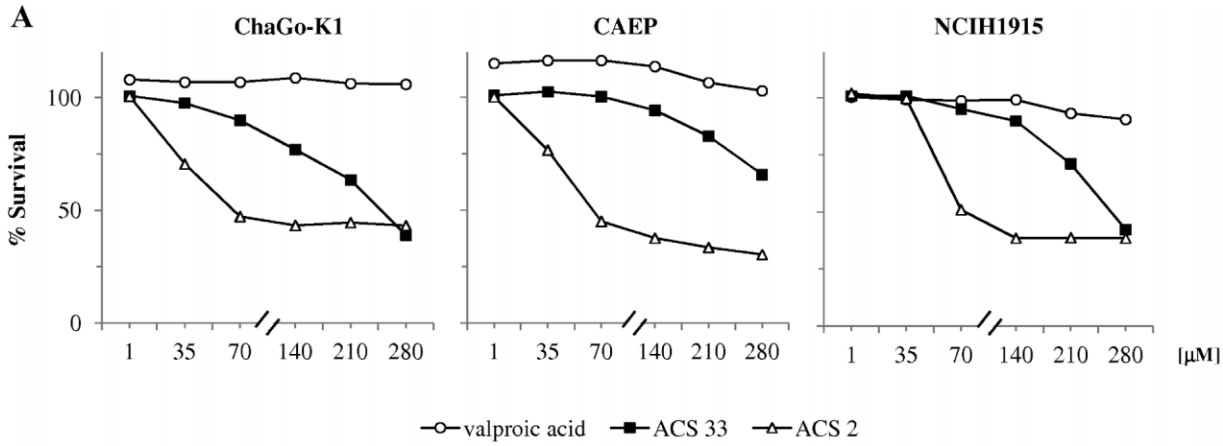

B

Drugs	IC_{50} values [μM]		
	ChaGo-K1	CAEP	NCIH1915
Valproic acid	n.r.*	n.r.	n.r.
ACS33	248	n.r.	261
ACS2	66,5	64,5	72

*not reached

Fig. 2. (A) Cytotoxic activity of valproic acid and of its derivatives ACS33 and ACS2 in human lung cancer cell lines ChaGo-K1, CAEP and NCIH1915 after a 72-h exposure. Each point indicates the mean of at least three experiments. Standard deviation (SD) never exceeded 5%. (B) Concentrations of valproic acid, ACS33, and ACS2 reduced cell survival by 50% (IC_{50}) in the panel of human lung cancer cell lines

noticeable in ChaGo-K1 cell line, the most resistant to ACS2, with cell survival almost totally suppressed. R-index values ranged from 1.9 in NCIH1915 to 5.6 in ChaGo-K1, with an intermediate value of 2.9 in CAEP cell line (Fig. 5).

To verify whether exposure to ACS2 induces chromatin decondensation, facilitating the cytotoxic action of cisplatin on DNA, we analyzed expression levels of the acetylated forms of the two histonic proteins H3 and H4 in CAEP cells. A 1.61- and 1.58-fold increment in expression levels of ac-H3 and ac-H4, respectively, was registered after a 4-h exposure to ACS 140 mM with respect to untreated samples (Fig. 6A). Similar results were observed in the other cell lines (data not shown). To confirm these findings, we used the acridine orange (AO) assay to analyze the different grades of susceptibility to denaturation of CAEP cells after exposure to ACS2 140 μM (Fig. 6B). Such an approach takes advantage of the fact that DNA in extended rather than condensed chromatin differs in susceptibility to denaturation, which in turn, correlates with chromatin condensation grades. Once again, we observed an increment of up to 30% in AO bound to ss DNA with respect to ds DNA, which is symptomatic of chromatin decondensation. Similar results were obtained in ChaGo-K1 and NCIH1915 lines (data not shown).

A preliminary investigation was also carried out into the effect of ACS2 combined with doxorubicin, another widely used anti-cancer agent. In this case the type of interaction observed was always additive, regardless of the drug schedule used (Table 2).

Discussion

Lung cancer, the most common cancer in the world, accounted for an estimated 960,000 new cases and 850,000 deaths among men and for 390,000 new cases and 330,000 deaths among women in 2008 (Boyle and Levin, 2008; Jemal et al., 2008). Unfortunately, the 5-year survival rate for NSCLC patients is less than 15%, indicating the urgency to identify innovative therapeutic strategies.

Histone deacetylases (HDACs) are a family of enzymes that regulate chromatin remodeling and gene transcription (Minucci and Pelicci, 2006), and there is growing interest in HDAC inhibitors as promising anticancer agents. Short chain fatty acids such as butyric and valproic acid were the first HDAC inhibitors to be identified as tumor growth inhibitors and inducers of apoptosis both in vitro and in vivo. However, they were found to have low potency, with IC_{50} in the millimolar range (Göttlicher et al., 2001). Despite such weak in vitro activity, VPA's anticancer mechanism of action has been investigated in preclinical models of skin, breast, colon, prostate and small cell lung cancer, and the drug is currently used in phase I–III clinical trials (Ma et al., 2009; Tan et al., 2010). Unfortunately, therapeutic doses of VPA are necessarily very high and cause limiting side-effects. An attempt to overcome the weak potency of VPA, due mainly to its inability to access the zinc cation in the HDAC active-site pocket, has been made by inserting sulfurated groups, selected amongst those known to be endowed with cancer chemopreventive activity and described

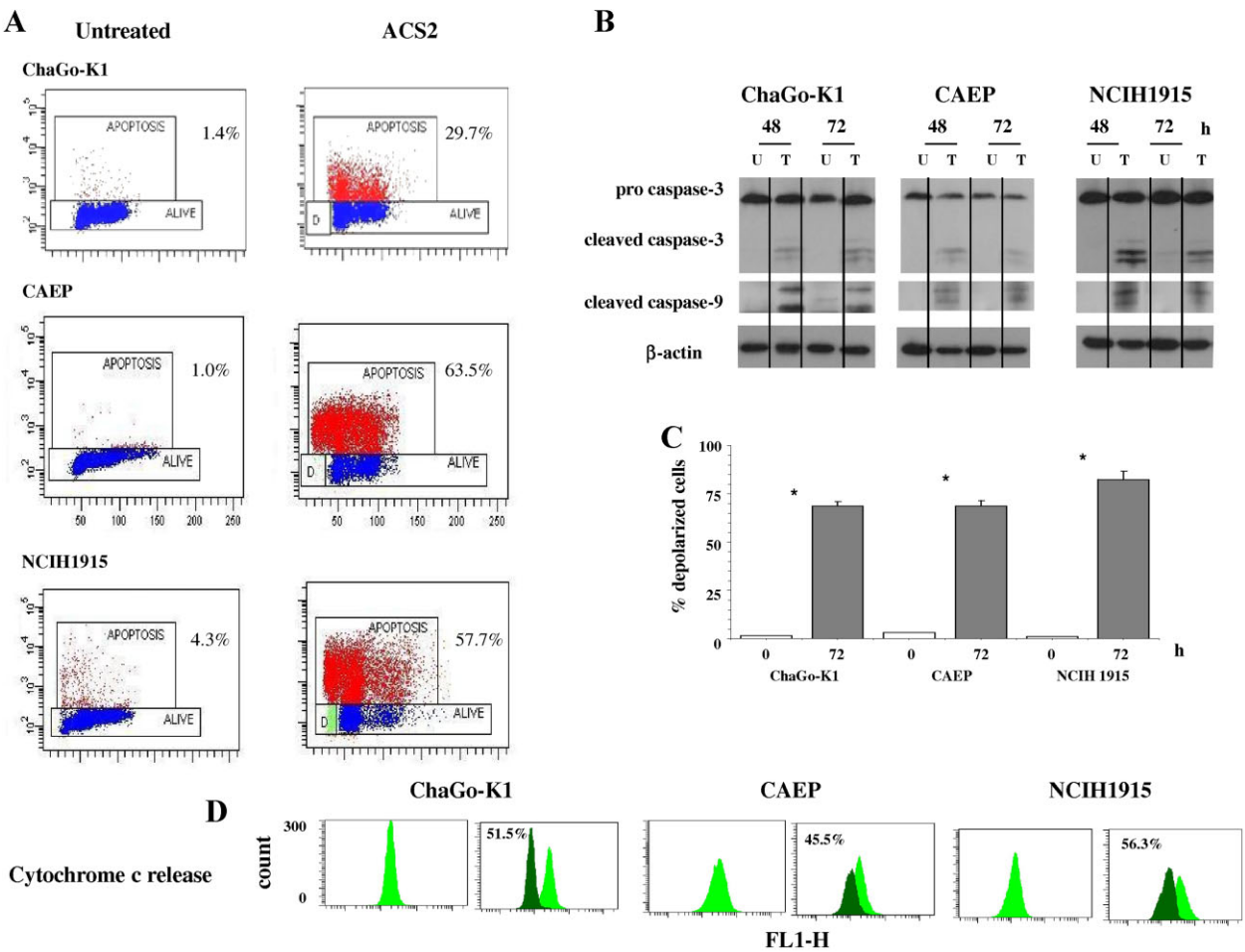

Fig. 3. (A) Analysis of apoptosis by cytometry using TUNEL assay in ChaGo-K1, CAEP, and NCIH1915 cells after a 72-h exposure to ACS2 140 μM. Each point indicates the mean of at least three experiments. Standard deviation (SD) never exceeded 5%. (B) Western blot analysis of apoptotic-related markers after a 48- and 72-h exposure to ACS2 140 μM. Images are representative of three experiments. (C) Percentage of mitochondrial membrane potential depolarization ($\Delta\Psi$) after a 72-h exposure to ACS2 140 μM. Samples were run in triplicate, and data are the average of three experiments. SD never exceeded 5%. (D) Representative image of cytochrome c release analysis after a 72-h exposure to ACS2 140 μM. Percentages reported are the average of three experiments. SD never exceeded 5%. *$P < 0.01$. [Color figure can be seen in the online version of this article, available at http://wileyonlinelibrary.com/journal/jcp]

as potent HDAC inhibitors, in the valproate moiety (Reddy et al., 1999; Nishino et al., 2003; Suzuki et al., 2004; Myzak and Dashwood, 2006; Myzak et al., 2006).

In the present work we evaluated the antitumor activity of valproic acid and its derivatives ACS33 and ACS2 bearing a thiosulfonate and dithiolthione moiety, respectively, in a panel of NSCLC cell lines. Both derivatives exhibited a much higher cytotoxic activity than that of the parent compound, with ACS2 proving to be the most effective drug, capable of reducing cell survival by 50% in all cell lines tested and at low concentrations. Such data are in agreement with those reported by Moody et al. (2010), although it must be pointed out that these authors used different cell lines and cell survival assays. The possibility of using ACS2 at low concentrations has therapeutic implications as it would eliminate the problem of side-effects of the valproate component, making ACS2 a potential "lead" compound for clinical development. On the basis of these data, we investigated the mechanism of action underlying the improved antitumor effect of ACS2 with respect to the parent compound, and discovered that the strong cytotoxic activity of ACS2 is largely due to its pro-apoptotic action observed in all cell lines. Our findings also showed that ACS2 triggers apoptotic machinery via the mitochondrial pathway, as highlighted by the strong mitochondrial membrane depolarization, cytoplasmatic cytochrome c release and caspase-9 and -3 cleavage. These data differ from the results obtained by Moody and coworkers who did not register apoptosis after exposure of NCI-H1299 cells to ACS2. Such a difference can probably be attributed to the specific experimental conditions used by the authors, i.e., the short exposure time (24 h) and the lower drug concentration (~28 μM) (Moody et al., 2010).

Matrix metalloproteinase-1 (MMP-1), an interstitial collagenase, plays an important role in the breakdown of extracellular matrix and mediates pathways of apoptosis, angiogenesis, and immunity. It has also been demonstrated that the overexpression of this enzyme is associated with tumor initiation, invasion, and metastasis of many types of human cancer including lung cancer (Murray et al., 1996; Sauter et al., 2008; Eck et al., 2009). Furthermore, a specific polymorphism of MMP-1 (MMP-1-1607 1G-to-2G) was recently found to be associated with susceptibility to both growth and progression of lung cancer (Liu et al., 2011).

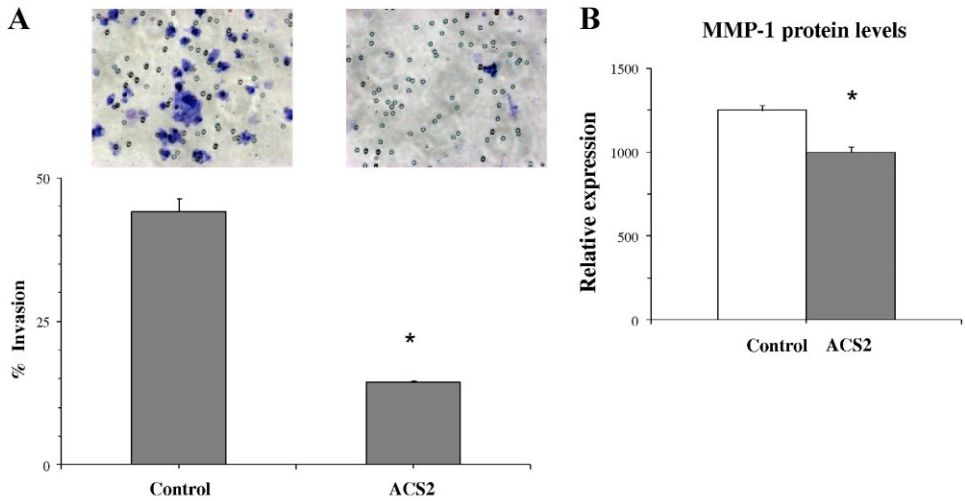

Fig. 4. (A) Effect of ACS2 (140 μM for 72 h) on invasive capacity of NCIH1915 cell line visualized by matrigel invasion assay. All assays were performed in triplicate and data were analyzed using the Student's *t*-test for unpaired observations. **P* < 0.05. (B) Expression levels of MMP-1 collagenase in NCIH1915 cell line before and after a 72-h exposure to ACS2 140 μM. The reproducibility of the relative mRNA expression was calculated from the results of two experiments in which the procedure was carried out on different retrotranscription products derived from the same mRNA sample. CV was always <5%. **P* < 0.05. [Color figure can be seen in the online version of this article, available at http://wileyonlinelibrary.com/journal/jcp]

In our study, we showed that ACS2 significantly reduces cell survival, diminishes the invasive capacity of NCIH1915, an established cell line obtained from a metastatic brain lesion, and downregulates MMP-1 expression. These data, together with the anti-angiogenic activity described by Isenberg et al. (2007), highlight the potential therapeutic effectiveness of ACS2 in advanced NSCLC where patient survival is very poor due to the high incidence of metastases (Minucci and Pelicci, 2006; Boyle and Levin, 2008).

Conventionally, NSCLC is treated with surgery in its early stages, while combination chemotherapy consisting of platinum-based regimens is standard practice in advanced disease. In our study we explored the potential for using ACS2 in combination with cisplatin and aimed to design an effective schedule based on the plasmatic half-life of both drugs. Our findings show that the simultaneous use of ACS2 and cisplatin for 6 h followed by a further 66-h exposure to ACS2 produced a highly tumoricidal effect in all cell lines tested starting from the lowest doses of both drugs. Furthermore, renal protection against the effect of cisplatin afforded by another dithiolethione (Park et al., 2008), in addition to the possibility of using low doses of both drugs, highlights a potentially good safety profile of the drug schedule. Finally, it can be hypothesized that the synergism between the two drugs is ascribable to the effect of ACS2 on chromatin remodeling through HDAC inhibition, which makes DNA less compact and more sensitive to cisplatin-induced damage. In fact, lower chromatin condensation was confirmed when an increase in acetylation of the two core histonic proteins (H3 and H4) was detected, a hallmark of chromatin relaxation, after a short exposure to ACS2 (Brownell and Allis, 1996). We also observed an increase in DNA susceptibility to denaturation after the same exposure time, which in turn correlates with chromatin decondensation (Darzynkiewicz, 1994).

Doxorubicin, a widely used antiblastic agent, is considered ineffective against a number of tumor types, including NSCLC, because of its narrow therapeutic range, outside of which side-effects such as severe cardiotoxicity have been observed (Ueda et al., 1987; Priebe et al., 1998; Singal et al., 2000; Awasthi et al., 2003; Folmer et al., 2007; Calcagno et al., 2008). A recent study has shown that deficiencies in H_2S synthesis may contribute to the pathogenesis of doxorubicin-induced cardiomyopathy and that administration of NaHS, an H_2S donor, ameliorates doxorubicin-related cardiac dysfunction by inhibiting oxidative stress injury (Su et al., 2009). The use of H_2S donors could therefore prove to be a promising therapeutic strategy to prevent doxorubicin-induced cardiotoxicity. We thus attempted to define an effective drug schedule for ACS2 and doxorubicin in our preclinical models, observing an additive interaction independently of the combination scheme used. These preliminary data are nevertheless interesting because of the potential cardiovascular protection provided by the H_2S component of ACS2. Further research is warranted into this specific area.

TABLE 1. Analysis of interactions between ACS2 and cisplatin

	Interaction type		
Drug schedule	NCIH1915	CAEP	ChaGo-K1
Pt (6 h) → 18-h w.o. → ACS2 (72 h)	Additive	Additive	Antagonistic
ACS2 (72 h) → Pt (6 h) → 18-h w.o.	Additive	Additive	Additive
ACS2 + Pt (6 h) → ACS2 (66 h)	Synergistic ($RI^* = 1.9$)	Synergistic ($RI_m = 2.9$)	Synergistic ($RI_m = 5.6$)

Pt, cisplatin; w.o., washout; *RI, R index >1.5 = synergism; RI < 0.5 = antagonism; RI >0.5 and < 1.5 = additivity.

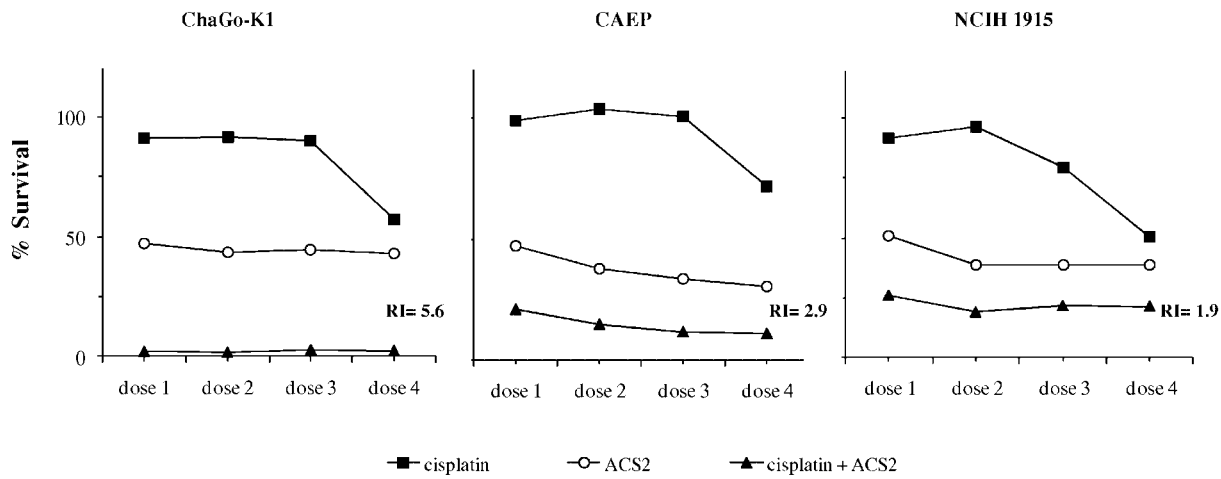

DRUG SCHEDULE	dose* 1	dose 2	dose 3	dose 4
Pt (6 h)→ 66-h w.o.	0.01	0.1	1	10
ACS2 (72 h)	70	140	210	280
ACS2 + Pt (6 h) → ACS2 (66 h)	0.01 (Pt); 70 (ACS2)	0.1 (Pt); 140 (ACS2)	1 (Pt); 210 (ACS2)	10 (Pt); 280 (ACS2)

* the drug doses are expressed in μM

Fig. 5. In vitro analysis of the synergistic interaction between cisplatin (Pt) and ACS2 when used in a concomitant treatment schedule (ACS2 + Pt for 6 h followed by ACS2 for a further 66 h). In the combination experiment, cisplatin was tested at concentrations of 0.01, 0.1, 1, and 10 μM, while ACS2 was used at concentrations of 70, 140, 210, and 280 μM. Each point indicates the mean of at least three experiments. SD never exceeded 5%.

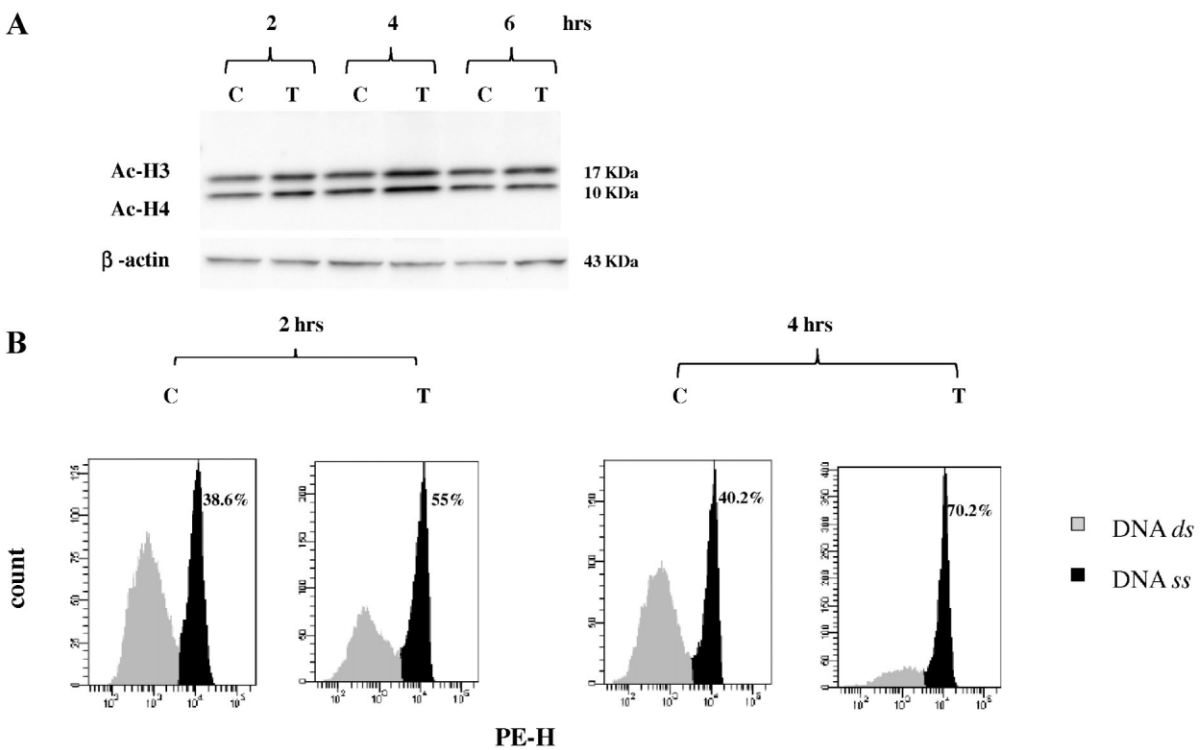

Fig. 6. (A) Expression changes of acetylated-histone 3 (ac-H3) and 4 (ac-H4) forms after different exposure times to ACS 2 140 μM in CAEP cells. C, control; T, treated; images are representative of two experiments. (B) Cytofluorimetric analysis of DNA sensitivity to denaturation using an acridine orange assay after a 2- and 4-h exposure to ACS2 140 μM. ds, double stranded; ss, single stranded. Percentages reported are the average of three experiments. SD never exceeded 5%.

TABLE 2. Analysis of interactions between ACS2 and doxorubicin

Drug schedule	Interaction type		
	NCIH 1915	CAEP	ChaGo-K1
DOXO (1 h) → 71 h w.o. → ACS2 (72 h)	Additive	Additive	Additive
ACS2 (72 h) → DOXO (1 h) → 71 h w.o.	Additive	Additive	Additive
ACS2 + DOXO (1 h) → ACS2 (71 h)	Additive (RI* = 1.5)	Additive	Additive

*RI, R index >1.5 = synergism; RI < 0.5 = antagonism; RI > 0.5 and <1.5 = additivity. ACS2 was used at concentrations of 70, 140, 210, and 280 μM, while doxorubicin (DOXO) was tested at concentrations of 0.005, 0.05, 0.5, and 5 μM.

In conclusion, our findings, in addition to demonstrating the increased cytotoxic activity of ACS33 and ACS2 with respect to valproic acid, highlight the strong pro-apoptotic activity of ACS2, a promising lead compound of this new class of HDAC inhibitors. Furthermore, we identified a highly effective combination schedule of ACS2 and cisplatin capable of inducing a synergistic interaction even when the two drugs are used at low concentrations. This increased efficacy is probably due to the modification induced by the valproate derivative on chromatin condensation, facilitating the establishment of cisplatin-DNA abducts. For these reasons, the VPA derivative ACS2 in combination with platinum compounds could represent a promising alternative to traditional chemotherapeutic regimens used for advanced lung cancer. Further in vivo studies are needed to confirm these results.

Acknowledgments

The authors thank Gráinne Tierney for editing the manuscript.

Literature Cited

Awasthi S, Singhal SS, Singhal J, Cheng J, Zimniak P, Awasthi YC. 2003. Role of RLIP76 in lung cancer doxorubicin resistance: II. Doxorubicin transport in lung cancer by RLIP76. Int J Oncol 22:713–720.

Baskar R, Bian J. 2011. Hydrogen sulfide gas has cell growth regulatory role. Eur J Pharmacol 656:5–9.

Baylin SB, Ohm JE. 2006. Epigenetic gene silencing in cancer-a mechanism for early oncogenic pathway addiction? Nat Rev Cancer 6:107–116.

Benavides GA, Squadrito GL, Mills RW, Patel HD, Isbell TS, Patel RP, Darley-Usmar VM, Doeller JE, Kraus DW. 2007. Hydrogen sulfide mediates the vasoactivity of garlic. Proc Natl Acad Sci USA 104:17977–17982.

Boyle P, Levin B, editors. 2008. World cancer report 2008. Lyon, France: IARC Press.

Brownell JE, Allis CD. 1996. Special HATs for special occasions: Linking histone acetylation to chromatin assembly and gene activation. Curr Opin Genet Dev 6:176–184.

Calcagno AM, Fostel JM, To KK, Salcido CD, Martin SE, Chewning KJ, Wu CP, Varticovski L, Bates SE, Caplen NJ, Ambudkar SV. 2008. Single-step doxorubicin-selected cancer cells overexpress the ABCG2 drug transporter through epigenetic changes. Br J Cancer 98:1515–1524.

Darzynkiewicz Z. 1994. Acid-induced denaturation of DNA in situ as a probe for chromatin structure. Methods Cell Biol 41:527–541.

Darzynkiewicz Z, Kapuscinski J. 1990. Acridine orange: A versatile probe of nucleic acids and other cell constituents. In: Melamed MR, Lindmo T, Mendelson ML, editors. Flow cytometry and sorting. 2nd ed. New York: Wiley – Liss. pp 291–314.

Duenas-Gonzalez A, Candelaria M, Perez-Plascencia C, Perez-Cardenas E, de la Cruz-Hernandez E, Herrera LA. 2008. Valproic acid as epigenetic cancer drug: Preclinical, clinical and transcriptional effects on solid tumors. Cancer Treat Rev 34:206–222.

Eck SM, Hoopes PJ, Petrella BL, Coon CI, Brinckerhoff CE. 2009. Matrix metalloproteinase-1 promotes breast cancer angiogenesis and osteolysis in a novel in vivo model. Breast Cancer Res Treat 116:79–90.

Feinberg AP, Tyco B. 2004. The history of cancer epigenetics. Nat Rev Cancer 4:143–153.

Feinberg AP, Ohlsson R, Henikoff S. 2006. The epigenetic progenitor origin of human cancer. Nat Rev Genet 7:21–33.

Folmer Y, Schneider M, Blum HE, Hafkemeyer P. 2007. Reversal of drug resistance of hepatocellular carcinoma cells by adenoviral delivery of anti-ABCC2 antisense constructs. Cancer Gene Ther 14:875–884.

Gasperi-Campani A, Roncuzzi L, Ricotti L, Lenzi L, Gruppioni R, Sensi A, Zini N, Zoli W, Amadori D. 1998. Molecular and biological features of two new human squamous and adenocarcinoma of the lung cell lines. Cancer Genet Cytogenet 107:11–20.

Göttlicher M, Minucci S, Zhu P, Krämer OH, Schimpf A, Giavara S, Sleeman JP, Lo Coco F, Nervi C, Pelicci PG, Heinzel T. 2001. Valproic acid derivatives: A novel class of HDAC inhibitors inducing differentiation of transformed cells. EMBO J 20:6969–6978.

Ibrahim T, Zoli W, Frassineti GL, Tesei A, Colantonio I, Monti M, Amadori D. 2005. Innovative sequence of docetaxel-gemcitabine based on preclinical data in the treatment of advanced non-small cell lung cancer: A phase I study. Lung Cancer 47:261–267.

Isenberg JS, Jia Y, Field L, Ridnour LA, Sparatore A, Del Soldato P, Sowers AL, Yeh GC, Moody TW, Wink DA, Ramchandran R, Roberts DD. 2007. Modulation of angiogenesis by dithiolethionemodified NSAIDs and valproic acid. Br J Pharmacol 151:142–151.

Jemal A, Siegel R, Ward E, Hao Y, Xu J, Murray T, Thun MJ. 2008. Cancer statistics, 2008. CA Cancer J Clin 58:71–96.

Jenuwein T, Allis CD. 2001. Translating the histone code. Science 293:1074–1080.

Kensler TW, Curphey TJ, Maxiutenko Y, Roebuck BD. 2000. Chemoprotection by organosulfur inducers of phase 2 enzymes: Dithiolethiones and dithiins. Drug Metabol Drug Interact 17:3–22.

Kern DH, Morgan CR, Hildebrand-Zanki SU. 1988. In vitro pharmacodynamics of 1-beta-D-arabinofuranosylcytosine: Synergy of antitumor activity with cisdiamminedichloroplatinum (II). Cancer Res 48:117–121.

Liu L, Wu J, Wu C, Wang Y, Zhong R, Zhang X, Tan W, Nie S, Miao X, Lin D. 2011. A functional polymorphism (-1607 1G→2G) in the matrix metalloproteinase-1 promoter is associated with development and progression of lung cancer. Cancer 117:5172–5181.

Ma X, Ezzeldin HH, Diasio RB. 2009. Histone deacetylase inhibitors: Current status and overview of recent clinical trials. Drugs 69:1911–1934.

Marchion DC, Bicaku E, Daud AI, Sullivan DM, Munster PN. 2005. Valproic acid alters chromatin structure by regulation of chromatin modulation proteins. Cancer Res 65:3815–3822.

Marks PA, Richon VM, Miller T, Kelly WK. 2004. Histone deacetylase inhibitors. Adv Cancer Res 91:137–168.

McIntyre J, Moral MA, Bozzo J. 2007. Combination therapy with valproic acid in cancer: Initial clinical approach. Drugs Future 32:45–50.

Minucci S, Pelicci PG. 2006. Histone deacetylase inhibitors and the promise of epigenetic (and more) treatments for cancer. Nat Rev Cancer 6:38–51.

Moody TW, Switzer C, Santana-Flores W, Ridnour LA, Berna M, Thill M, Jensen RT, Sparatore A, Del Soldato P, Yeh GC, Roberts DD, Giaccone G, Wink DA. 2010. Dithiolethione modified valproate and diclofenac increase E-cadherin expression and decrease proliferation of non-small cell lung cancer cells. Lung Cancer 68:154–160.

Murray GI, Duncan ME, O'Neil P, Melvin WT, Fothergill JE. 1996. Matrix metalloproteinase-1 is associated with poor prognosis in colorectal cancer. Nat Med 2:461–462.

Myzak MC, Ho E, Dashwood RH. 2006. Dietary agents as histone deacetylase inhibitors. Mol Carcinog 45:443–446.

Myzak MC, Dashwood RH. 2006. Histone deacetylases as targets for dietary cancer preventive agents: Lessons learned with butyrate, diallyl disulfide, and sulforaphane. Curr Drug Targets 7:443–452.

Nishino N, Jose B, Okamura S, Ebisusaki S, Kato T, Sumida Y, Yoshida M. 2003. Cyclic tetrapeptides bearing a sulfhydryl group potently inhibit histone deacetylases. Org Lett 5:5079–5082.

Park HM, Cho JM, Lee HR, Shim GS, Kwak MK. 2008. Renal protection by 3H-1,2-dithiole-3-thione against cisplatin through the Nrf2-antioxidant pathway. Biochem Pharmacol 76:597–607.

Parkin DM, Bray F, Ferlay J, Pisani P. 2005. Global cancer statistics, 2002. CA Cancer J Clin 55:74–108.

Perrino E, Cappelletti G, Tazzari V, Giavini E, Del Soldato P, Sparatore A. 2008. New sulfurated derivatives of valproic acid with enhanced histone deacetylase inhibitory activity. Bioorg Med Chem Lett 18:1893–1897.

Priebe W, Krawczyk M, Kuo MT, Yamane Y, Savaraj N, Ishikawa T. 1998. Doxorubicin- and daunorubicin-glutathione conjugates, but not unconjugated drugs, competitively inhibit leukotriene C4 transport mediated by MRP/GS-X pump. Biochem Biophys Res Commun 247:859–863.

Reddy BS. 1996. Chemoprevention of colon cancer by minor dietary constituents and their synthetic analogues. Prev Med 25:48–50.

Reddy BS, Kawamori T, Lubet R, Steele V, Kelloff G, Rao CV. 1999. Chemopreventive effect of S-methylmethane thiosulfonate and sulindac administered together during the promotion/progression stages of colon carcinogenesis. Carcinogenesis 20:1645–1648.

Romanelli S, Perego P, Pratesi G, Carenini N, Tortoreto M, Zunino F. 1998. In vitro and in vivo interaction between cisplatin and topotecan in ovarian carcinoma systems. Cancer Chemother Pharmacol 41:385–390.

Rosetti M, Tesei A, Ulivi P, Fabbri F, Vannini I, Brigliadori G, Amadori D, Bolla M, Zoli W. 2006. Molecular characterization of cytotoxic and resistance mechanisms induced by NCX 4040, a novel NO- NSAID, in pancreatic cancer cell lines. Apoptosis 11:1321–1330.

Ruggeri BA, Robinson C, Angeles T, Wilkinson J IV, Clapper ML. 2002. The chemopreventive agent oltipraz possesses potent antiangiogenic activity in vitro, ex vivo, and in vivo and inhibits tumor xenograft growth. Clin Cancer Res 8:267–274.

Sauter W, Rosenberger A, Beckmann L, Kropp S, Mittelstrass K, Timofeeva M, Wölke G, Steinwachs A, Scheiner D, Meese E, Sybrecht G, Kronenberg F, Dienemann H. LUCY-Consortium, Chang-Claude J, Illig T, Wichmann HE, Bickeböller H, Risch A, 2008. Matrix metalloproteinase 1 (MMP1) is associated with early onset lung cancer. Cancer Epidemiol Biomarkers Prev 17:1127–1135.

Singal PK, Li T, Kumar D, Danelisen I, Iliskovic N. 2000. Adriamycin-induced heart failure: Mechanism and modulation. Mol Cell Biochem 207:77–86.

Skehan P, Storeng R, Scudiero D, Monks A, McMahon J, Vistica D, Warren JT, Bokesch H, Kenney S, Boyd MR. 1990. New colorimetric cytotoxicity assay for anticancer-drug screening. J Natl Cancer Inst 82:1107–1112.

Spiro SG, Silvestri GA. 2005. One hundred years of lung cancer. Am J Respir Crit Care Med 172:523–529.

Spiro SG, Porter JC. 2002. Lung cancer - where are we today? Current advances in staging and nonsurgical treatment. Am J Respir Crit Care Med 166:1166–1196.

Suzuki T, Kouketsu A, Matsuura A, Kohara A, Ninomiya S, Kohda K, Miyata N. 2004. Thiol-based SAHA analogues as potent histone deacetylase inhibitors. Bioorg Med Chem 14:3313–3317.

Su YW, Liang C, Jin HF, Tang XY, Han W, Chai LJ, Zhang CY, Geng B, Tang CS, Du JB. 2009. Hydrogen sulfide regulates cardiac function and structure in adriamycin-induced cardiomyopathy. Circ J 73:741–749.

Tan J, Cang S, Ma Y, Petrillo RL, Liu D. 2010. Novel histone deacetylase inhibitors in clinical trials as anti-cancer agents. Hematol Oncol 3:5.

Ueda K, Cardarelli C, Gottesman MM, Pastan I. 1987. Expression of a full-length cDNA for the human "MDR1" gene confers resistance to colchicine, doxorubicin, and vinblastine. Proc Natl Acad Sci USA 84:3004–3008.

Wedel SA, Sparatore A, Soldato PD, Al-Batran SE, Atmaca A, Juengel E, Hudak L, Jonas D, Blaheta RA. 2008. New histone deacetylase inhibitors as potential therapeutic tools for advanced prostate carcinoma. J Cell Mol Med 12:2457–2466.

Witt O, Deubzer HE, Milde T, Oeheme I. 2008. HDAC family: What are the cancer relevant targets? Cancer Lett 277:8–21.

Zoli W, Ricotti L, Tesei A, Barzanti F, Amadori D. 2001. In vitro preclinical models for a rational design of chemotherapy combinations in human tumors. Crit Rev Oncol Hematol 37:69–82.